Chapter 14

VALENCE BAND ORDERING AND MAGNETO-OPTICAL PROPERTIES OF FREE AND BOUND EXCITONS IN ZnO

A.V. Rodina[1], M. Strassburg[2], M. Dworzak[2], U. Haboeck[2], A. Hoffmann[2], H. R. Alves[3], A. Zeuner[3], D. M. Hofmann[3], and B. K. Meyer[3]
[1]*A.F. Ioffe Physico-Technical Institute, St.-Petersburg, Russia;* [2]*Institute of Solid State Physics, Technical University of Berlin, Berlin, Germany;* [3]*I. Physics Institute, Justus-Liebig-University Giessen, Giessen, Germany*

Abstract: The Zeeman splitting of free and bound excitons is analysed theoretically for both Γ_7 and Γ_9 symmetries of the upper valence band. The Zeeman splitting of the Γ_7 (Γ_9) holes in magnetic field parallel to the hexagonal ***c*** axes of the crystal is found to be smaller (larger) than the Zeeman splitting of the electrons. The magnetic-field dependence of the bound exciton optical transition energies measured in the Faraday geometry with right and left circular polarized light can be well described with Γ_7 as well as with Γ_9 holes. However, the fitting of the experimental dependence of the Zeeman splitting on the angle between magnetic field and ***c*** axis proves the Γ_7 symmetry of the holes involved in all low temperature transitions and thus of the upper valence band in bulk ZnO. The determined parameters are in excellent agreement with known experimental data on the fine structure of the free exciton ground state in ZnO. The hole *g*-factors determined for excitons bound to an ionized and neutral impurity centers are close to each other and to the *g*-factor calculated for the Γ_7 hole in the free exciton ground state. This points to a donor character of the neutral impurity centers. This conclusion is confirmed by temperature dependent magneto-transmission and magneto-luminescence measurements.

Key words: Photoluminescence, magneto-luminescence, Zeeman effect, g-factor, excitons, valence band symmetry

1. INTRODUCTION

Bulk ZnO is a direct band gap wurtzite semiconductor with the valence band maximum split by the crystal field and spin-orbit interaction. The

N.H. Nickel and E. Terukov (eds.),
Zinc Oxide – A Material for Micro- and Optoelectronic Applications, 159–170.

symmetry of the upper valence subband (A-subband) has been the subject of controversy (Γ_9 or Γ_7 character) for more than 40 years.[1-15] Based on the polarization properties of the free exciton transitions, the inverted ordering of the valence subbands as shown in Figure 1(a) was first suggested by Thomas[1] and supported later in many articles.[3-7,11-18,21] However, different argumentation led some researches[2,8-10,19,20] to the conclusion that the ordering of valence subbands in ZnO is the same as in other wurtzite semiconductors like GaN, CdSe, CdS (see Figure 1(b)).

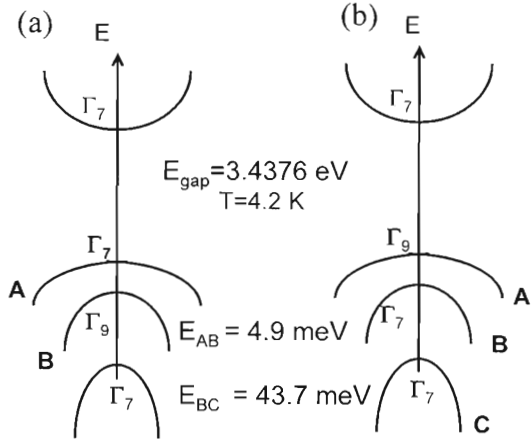

Figure 1. Energy band structure and the symmetry of the free exciton ground state in wurtzite-type semiconductors for (a) ZnO and (b) GaN, CdSe, CdS.

Magneto-optical studies are a powerful tool to distinguish the symmetry of the free and bound exciton states.[5-8,14-21] Unfortunately, most of the magneto-optical investigations in ZnO were incomplete and allowed both interpretations concerning the symmetry of the holes involved. For example, recent magneto-optical studies[8] of the free A exciton fine structure were interpreted with the assumption of the Γ_9 symmetry for the valence band maximum, while the more elaborated theoretical analysis[11] enabled the explanation of the same date applying the Γ_7 symmetry for the A valence band. To resolve this controversy, detailed theoretical and experimental studies of the magneto-optical properties of bound excitons in bulk ZnO were undertaken.[14] In this paper we show that the detailed comparison between the theoretical predictions and the experimentally observed Zeeman behavior of free excitons and bound exciton complexes in bulk ZnO confirms the Γ_7 symmetry of the upper valence subband.

2. THEORY

The inverted ordering of the valence subbands (Fig. 1(a)) can be understood in terms of an effective negative spin-orbit splitting. The first-principles band structure calculations of Ref. 11 confirmed the inverted ordering in bulk ZnO. It was found that the negative spin-orbit coupling arises from the contribution of the lower lying Zn *3d* bands. The optimal value for the Zn *3d* bands position was derived which gives good agreement with the basic valence band splittings.[11] A self consistent set of the effective mass parameters obtained from these band structure calculations was used in the analysis of the exciton binding energies and effective *g* values.[11]

In Figure 2 we sketch all possible transitions from the free exciton and from the exciton bound to the ionized impurity center corresponding to the calculated values[11] of the hole effective *g*-factors. We consider the holes from the Γ_7 (case (a)) and Γ_9 (case (b)) valence bands. We take in account only the short-range exchange interaction in Fig. 2 and do not consider the long range exchange interaction or polariton effects. The zero field exchange splitting between the Γ_1 and Γ_2 exciton states is neglected in Fig. 2 (a) as it is known to be small in ZnO.[11] The zero field spin-exchange splitting of the Γ_1/Γ_2 and Γ_5 exciton states (case (a)) or Γ_6 and Γ_5 exciton states (case (b)) is about 0.95 meV[23] and governs the Zeeman behavior in the magnetic field perpendicular to the ***c*** axis. In the magnetic field parallel to the ***c*** axis the linear Zeeman splitting of the Γ_5 exciton state is expected. The Γ_6 state and the Γ_1/Γ_2 states mixed by the magnetic field also show the linear splitting. The splitting is given by

$$\mu_B B g_{exc} = \mu_B B(g_h^{//} \pm g_e), \qquad (1)$$

where μ_B is the (positive) value of the Bohr magneton, $g_e=1.95$ is the electron (isotropic) effective g-factor and the calculated values of the hole effective *g* factor are $g_h^{//}(\Gamma_7) = -1.4\pm0.15$ for the Γ_7 hole in the exciton ground state and $g_h^{//}(\Gamma_9) = 3.0\pm0.15$ for the Γ_9 hole. The resulting values of the exciton effective *g*-factors g_{exc} for all states are shown in the Figure 2. For the transitions allowed with $\boldsymbol{E} \perp \boldsymbol{c}$ the g_{exc} values are positive in both (a) and (b) cases. Therefore in the $\boldsymbol{B} // \boldsymbol{c} // \boldsymbol{k}$ configuration the upper-energy state is expected to be active for the right-circular polarized light σ^+. In the $\boldsymbol{k} \perp \boldsymbol{c}$ configuration, the transitions with $\boldsymbol{E} // \boldsymbol{c}$ are allowed in the case (a); in the case (b) they are forbidden but might be observed due to high-order perturbations. The calculated g_{exc} values for the Γ_7 hole (case (a)) in $\boldsymbol{B} // \boldsymbol{c}$ describe well the experimental data reported in Ref. 8 for the free exciton ground state in both $\boldsymbol{E} \perp \boldsymbol{c}$ and $\boldsymbol{E} // \boldsymbol{c}$ polarization. We discuss the

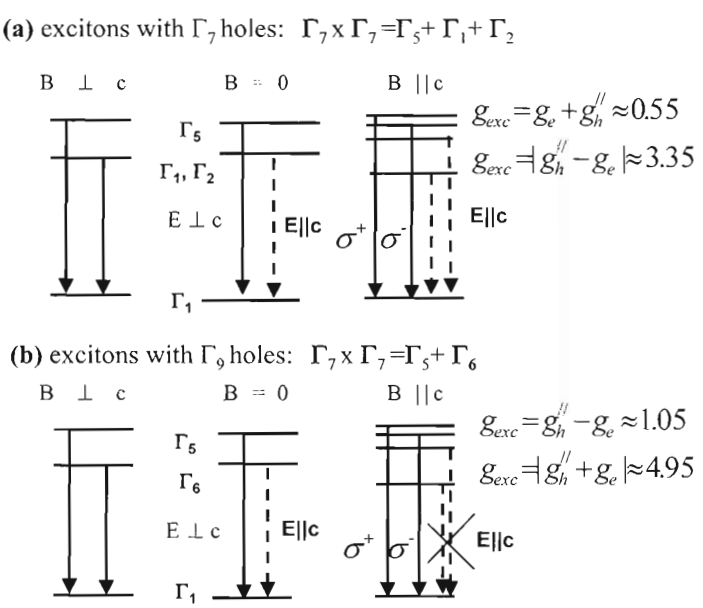

Figure 2. Level schemes and selection rules for the ionized bound exciton transitions.

experimentally Zeeman splitting of the ionized donor bound exciton complex in the next section.

In Figure 3 we sketch all possible transitions for excitons bound to neutral impurities considering the holes from the Γ_7 (cases (a), (c)) and Γ_9 (cases (b), (d)) valence bands. In the case of a donor bound exciton complex (Fig. 3 (a) and (b)), the spins of two electrons are anti-parallel and the Zeeman splitting of the excited (D_0, X) state is determined by the anisotropic hole effective g factor (g_h), while the splitting of the ground D_0 state is given by g_e. In the case of an acceptor bound exciton complex (Fig. 3 (c) and (d)), two holes have the same symmetry and anti-parallel spins. Hence, the splitting of the excited (A_0, X) state is determined by g_e, while the ground A_0 state splits according to g_h. For the holes in the exciton states we use in Fig. 3 (a) and (b) the g values calculated in Ref. 11. For the holes in the acceptor ground states we use in Fig. 3 (c) and (d) the values calculated using the theory developed in Ref. 24 with effective mass Luttinger parameters from Ref. 11.

Our calculations show that the Zeeman splitting of the Γ_7 (Γ_9) holes in ***B//c*** determined by $|g_h^{//}|$ is smaller (larger) than the Zeeman splitting of the electrons determined by g_e. For the arbitrary angle Θ between the ***c*** axis and the direction of the magnetic field the absolute value of the hole anisotropic g factor is given by[22]

$$g_h(\Theta) = \sqrt{|g_h^{//}|^2 \cos^2\Theta + |g_h^{\perp}|^2 \sin^2\Theta} \qquad (2)$$

Therefore, for the Γ_7 holes the Zeeman splitting in any magnetic field remains always smaller than the Zeeman splitting of the electrons. In contrary, for the Γ_9 holes some critical angle Θ_{cr} should exist so that $g_h(\Theta_{cr})=g_e$, and $g_h(\Theta)>g_e$ for $0^\circ \le \Theta < \Theta_{cr}$ and $g_h(\Theta)< g_e$ for $90^\circ \ge \Theta > \Theta_{cr}$. Examination of the selection rules for optical transitions in the ***B // c // k*** configuration shows that the upper-energy transition is expected to be active for the right-circular polarized light σ^+ for all cases presented in Fig. 3 cases.

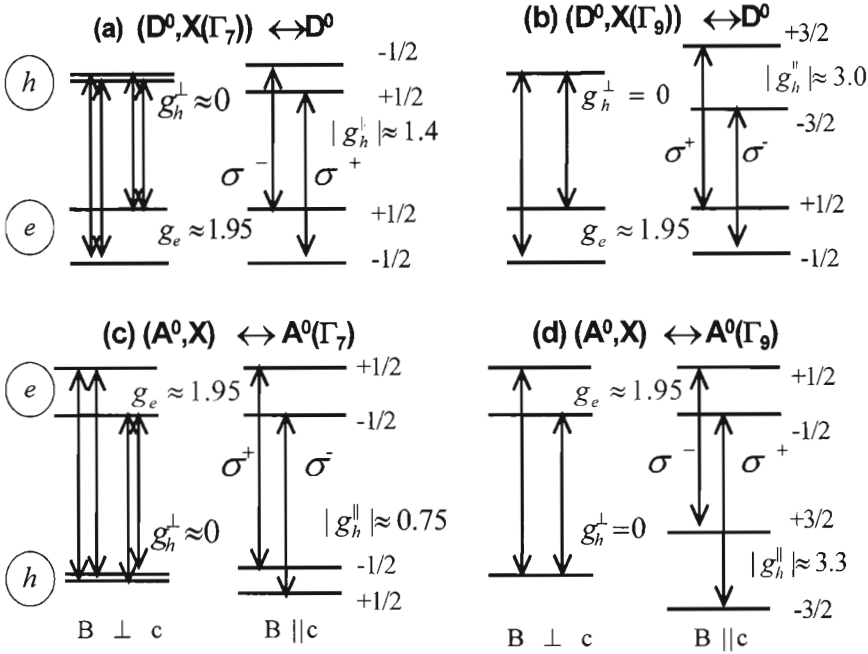

Figure 3. Level schemes and selection rules for neutral bound exciton transitions.

3. EXSPERIMENTAL SETUP AND SAMPLE CHARACTERIZATION

We used nominally undoped (as grown from Eagle-Picher, see for details Ref. 15) and nitrogen doped bulk ZnO crystals. A nitrogen doped ZnO:N sample was prepared from the as grown one by ion implantation (2 MeV,10^{13} cm^{-2}) followed by a thermal annealing process at 900 °C for 15 min (see also Ref. 15).

The magneto-PL measurements were performed at liquid helium temperature in a split-coil magnetocryostat allowing the variation of both temperature (2–300 K) and magnetic field (0–5 T). For some measurements, a second split-coil magnetocryostat was applied providing magnetic fields up to 15 T. Photoluminescence was excited by the 325 nm line of a HeCd laser. A 450 W XBO lamp was used as excitation source for the transmission investigations. The spectral resolution of the detection system was better than 0.15 meV for the 5 T cryostat and >0.3 meV for the 15 T cryostat.

The magneto-PL and magneto-PT measurements were performed in Faraday configuration (magnetic field $\boldsymbol{B}$ parallel to the $\boldsymbol{c}$ axis of the crystal and parallel to the $\boldsymbol{k}$ vector of the detected light) and in Voigt configuration ($\boldsymbol{B} \perp \boldsymbol{k}$). Additionally, the angles between $\boldsymbol{B}$ and $\boldsymbol{c}$ axes were varied from 0 to 90° at fixed magnetic field of 5 T. The circular polarization of the light (σ^+ and σ^-) in the Faraday configuration was analyzed using l/4 plate and linear polarizer. Additionally, PL spectra with $\boldsymbol{B} \perp \boldsymbol{c}$, $\boldsymbol{k} \perp \boldsymbol{c}$ and $\boldsymbol{E} \parallel \boldsymbol{c}$ were recorded for the ZnO:N. Temperature-dependent measurements reveals the thermalization behavior of the Zeeman split components in the emission and transmission spectra.

The zero-field PL spectra of the as grown (nominally undoped) ZnO and nitrogen doped ZnO:N are shown in Figs. 4(a) and 4(b), respectively. Only the lines that will be discussed in this paper in details are marked (for other lines see Ref. 14,15). The strongest line in the as grown ZnO (see Fig. 4 (a)) is the I_4 (368.59 nm or 3.3628 eV). We attribute the I_4 transition as an exciton bound to a neutral shallow H donor that can be easily removed by an annealing process.[15,25] Indeed, the I_4 PL line is absent in ion implanted ZnO:N (see Fig. 4(b)). This is because of the post annealing processes at 900 °C included in the doping procedure. The PL spectrum of ZnO:N is dominated by two lines: a new line I_2 (368.07 nm or 3.3676 eV) and the I_9 transition. The latter considerably gains in intensity compared to the undoped ZnO. The wavelengths of the lines are given here in air with an accuracy of 0.02 nm and have been transformed into the respective wavelength values in vacuum before calculating the transition energies.

4. ZEEMAN BEHAVIOR OF THE BOUND EXCITON COMPLEXES: EXPERIMENTAL DATA AND DISCUSSION

Figure 5 presents the magneto-PL spectra in the energy region of the I_2 transition for the ZnO:N for Faraday configuration (a), Voigt configuration (c) and for the different angles between the magnetic field direction and the

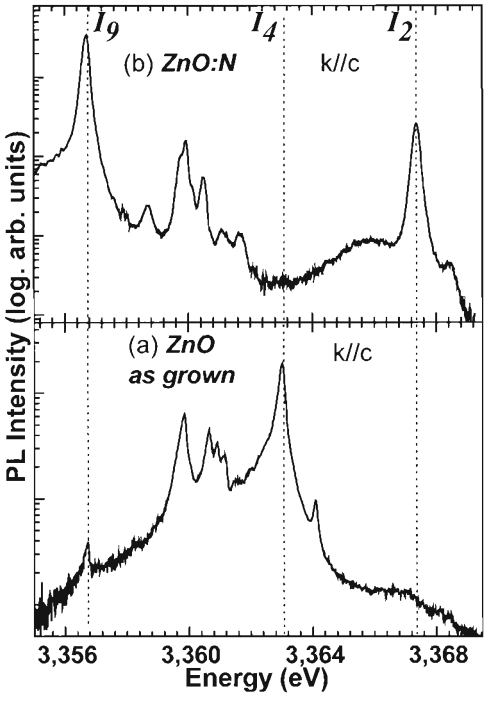

Figure 4. Photoluminescence spectra of undoped as grown ZnO (a) and nitrogen doped ZnO:N (b) at 4.2 K.

c axis at $B = 5$ T (b). The most important feature of the spectra in Figures 2 (b) and (c) is the appereance of a new transition line at an energy about 1 meV below I_2. This I_3 transition (368 18 nm or 3 3666 eV in zero field as determined by the extrapolating procedure) is forbidden in $\boldsymbol{B}$ // k // $\boldsymbol{c}$, $\boldsymbol{E} \perp \boldsymbol{c}$ geometry but has been also observed in parallel magnetic field with the light polarized along the c axis ($\boldsymbol{E}$ // $\boldsymbol{c}$, $\boldsymbol{k} \perp \boldsymbol{c}$ configuration). Such behavior leads to the conclusion that the I_2 and I_3 transitions originate from excitons bound to an ionized impurity. The stability of such complex in semiconductors strongly depends on the ratio of electron and hole effective masses.[26] In the case of ZnO, the single band isotropic mass approximation predicts the existence of the excitons bound to ionized donors.[23] Next, the presence of acceptors in the ZnO:N may induce the ionization of the shallow donors[26] as in the case of Li and Na doped ZnO.[19] Therefore, we attribute the I_2 and I_3 lines in the doped ZnO:N to transitions of excitons bound to respective ionized donors ((D^+, $X(\Gamma_7)$) complex). The value of the zero-field spin-exchange splitting is 0.98 meV, in a good agreement with Refs. 19,23.

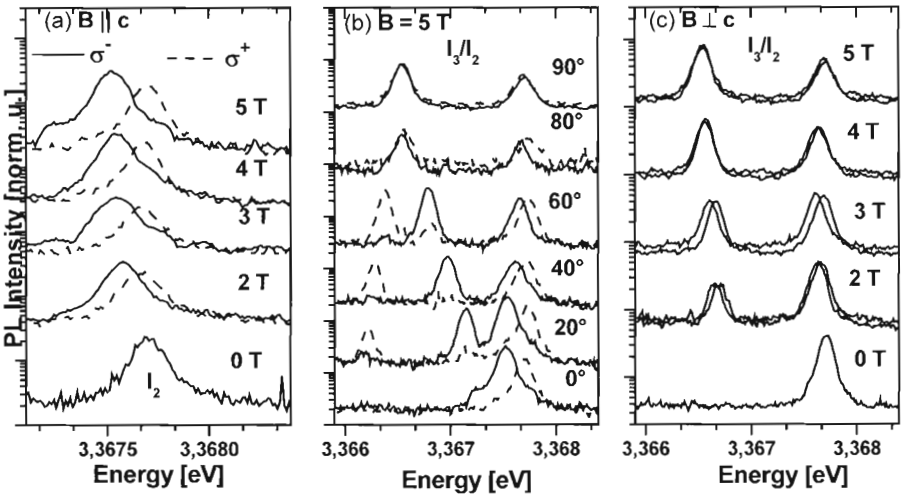

Figure 5. Photoluminescence spectra of ZnO:N in the energy region of the I2/I3 lines at 4:2 K for different magnetic fields in Faraday configuration (case (a): B // k // c, E ⊥ c) and Voigt configuration (case (c): B ⊥ c, k // c, E ⊥ c), and for different angles between the c axis and the direction of the magnetic field B at 5 T (case (b)).

The magnetic field and angular dependencies of the emission lines I_2 and I_3 allow us to determine the symmetry and the g values of the valence band hole involved in the corresponding bound excitons.[14,15] The magnetic field $\boldsymbol{B} \,//\, \boldsymbol{c}$ linearly splits the I_2 transition (allowed in $\boldsymbol{E} \perp \boldsymbol{c}$ configuration) as well as the I_3 transition (allowed in $\boldsymbol{E} \,//\, \boldsymbol{c}$ configuration). The upper-energy component of the I_2 line is active for the right-circular polarized light (see dashed line in Fig. 5 (a)) as predicted in Fig. 2. The linear splitting of the I_2 line in $\boldsymbol{B} \,//\, \boldsymbol{c}$ can be described with the positive exciton effective g- factor $g_{exc} = 0.71$ that is close to the calculated values in Fig.2 (a) and (b). However, the experimental value $g_{exc} = 2.66$ determined for the I_3 line is in better agreement with the expected value for the Γ_7 holes (case (a) in Fig. 2) and differs significantly from the respective value in case (b). Furthermore, from the fitting of the angular dependence of the transition energies[14,15] we obtained $g_h^{//} = -1.24$ in the excellent agreement with the calculated value for the Γ_7 hole in the exciton ground state. This demonstrates that the hole in the lowest exciton state and thus the upper A valence subband in ZnO also have the Γ_7 symmetry.

The Zeeman behavior of the emission lines from I_4 to I_9 is different from that of the I_2/I_3 lines. Their linear splitting in $\boldsymbol{B} \perp \boldsymbol{c}$ indicates transitions originating from excitons bound to neutral impurities. We discuss the emission lines I_9 and I_4 in detail. These lines represent the dominant

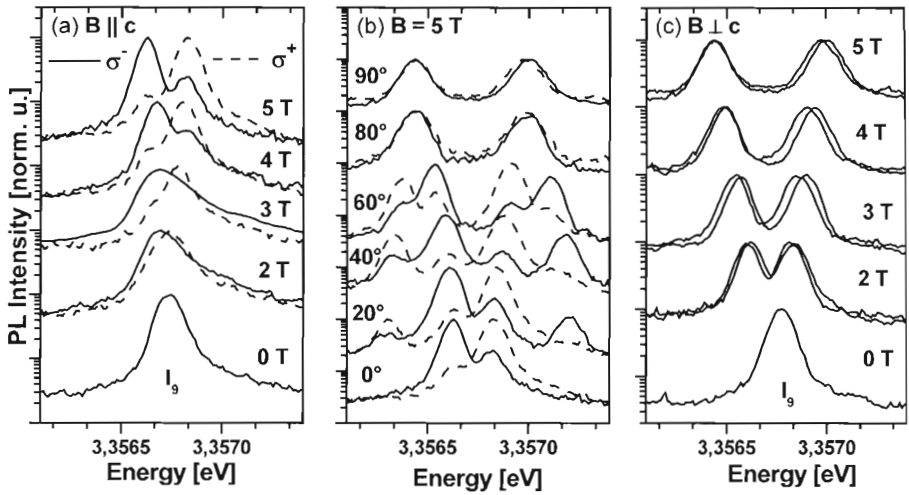

Figure 6. Photoluminescence spectra of ZnO:N in the energy region of the I9 line at 4:2 K. Cases (a), (b) and (c) are the same as in Fig. 5.

recombination in ZnO:N and as grown ZnO bulk crystals, respectively, and are spectrally resolved from the other observed emission lines. Figure 6 presents the magneto-PL spectra in the energy region of the I_9 transition for the ZnO:N, the Zeeman behavior of this line and the I_4 in the undoped ZnO is very similar. The transitions allowed for $\boldsymbol{E} \perp \boldsymbol{c}$ split with magnetic fields parallel and perpendicular to the $\boldsymbol{c}$ axis. The upper Zeeman split energy component in $\boldsymbol{B} // \boldsymbol{c} // \boldsymbol{k}$ configuration is active in σ^- polarization (see Fig. 6 (a)) as predicted for all cases in Fig. 3 (a-d). Four transition components can be distinguished for an arbitrary angle Θ between the direction of the magnetic field and the $\boldsymbol{c}$ axis.

The B-field dependencies up to 5 T of the I_4 transition energies in $\boldsymbol{B} \perp c$ and $\boldsymbol{B} // \boldsymbol{c}$ are shown in Figure 7 together with the angular dependence at B = 5 T. These dependencies can be described as

$$E(B,\Theta) = E_0 \pm 1/2\mu_B B(g_e \pm g_h(\Theta)), \qquad (3)$$

where E_0 is the zero field transition energy and $g_h(\theta)$ is given by Eq. (2). For the Γ_9 holes the $g_h^{\perp} = 0$ by the symmetry and the Eq. (3) leads to the linear dependence of $E(B,\Theta)$ on $cos(\Theta)$ (see dashed lines in Fig. 7 (b)). For the Γ_7 holes in ZnO the value of $g_h^{\perp} \approx 0$ and the nonlinear behavior of $E(B,\Theta)$ on $cos(\Theta)$ can not be detected as well (see solid lines in Fig. 7 (b)). However, the symmetry of the holes can be unambiguously established by the analysis of the angular dependence in Fig. 7 (b). Indeed, no critical

angle θ_{cr} corresponding to $g_h(\Theta_{cr})=g_e$ and no respective crossing of the transition energies expected for the Γ_9 holes (see dashed lines in Fig. 7 (b)) was observed. The excellent agreement between experimental data and theoretical modeling is possible if and only if we assume that the hole g factor is smaller than electron's g factor: $|g_h^{//}| < g_e$. Together with the selection rules observed in ***B*** // ***c*** // ***k*** configuration this corresponds to the holes of the Γ_7 symmetry. The values of the electron and hole effective g factors used for the fitting (solid curves) are $g_e = 1.97$, $g_h^{//} = -1.21$ and $g_h^{\perp} = 0.1$ for the I_4 in Fig. 7 and $g_e = 1.86$, $g_h^{//} = -1.27$ and $g_h^{\perp} = 0.06$ for the I_9 line[14].

The values of $g_h^{//}$ derived for the I_4 and I_9 lines are very close to the $g_h^{//} = -1.24$ obtained for the hole involved in the exciton bound to ionized donor and to the g factor of the hole in $1S$ free exciton state.[5,7,11] On the other hand, the expected $g_h^{//}$ values of the holes involved in the acceptor bound exciton transitions differ significantly from the g values of the holes involved into excitons bound to ionized or neutral donors. This is similar to the situation found in CdS.[22] Therefore we conclude that both I_4 and I_9 transitions should be assigned to the $(D_0;X_A(\Gamma_7))$ complex rather than to the $(A_0(\Gamma_7);X_A(\Gamma_7))$.

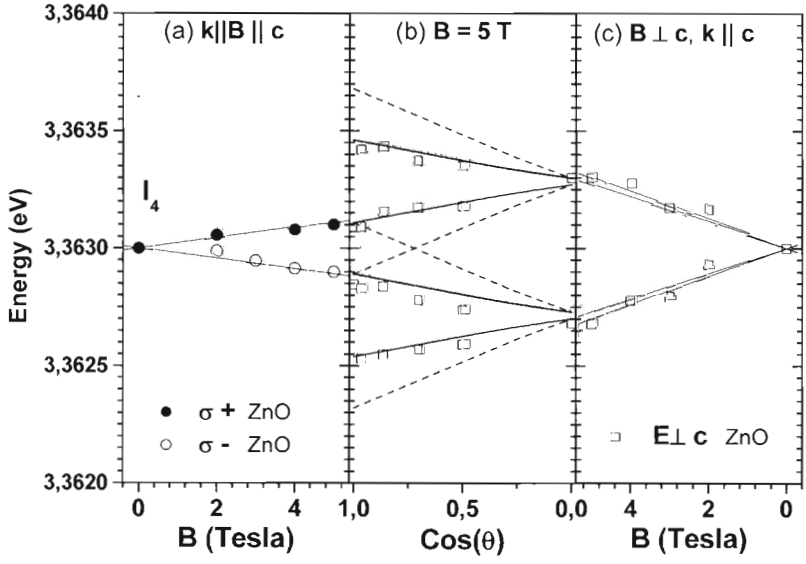

Figure 7. Zeeman splitting of the bound exciton line I4. Case (a): B // k // c, E ⊥ c. Case (c): B ⊥ c, k // c, E ⊥ c. Case (b): the angular dependence for B = 5 T. Symbols are experimental data measured with circular polarized light (σ^+ and σ^-) and with unpolarized light (E ⊥ c) as denoted in the Figure, and lines are fits. For the fits the hole is assumed to be of Γ7 symmetry with $|g_h^{\perp}| < g_e$ (solid lines) and of Γ9 symmetry with $|g_h^{//}| > g_e$ (dashed lines).

This conclusion is supported by the analysis of the thermalization properties of the I_4 and I_9 lines[14] in the temperature dependent emission and transmission spectra and by the observation of the two electron satellite transitions for these lines.[15,21,25]

5. CONCLUSION

The inverted $\Gamma_7(A)$, $\Gamma_B(B)$, $\Gamma_7(C)$ ordering of the valence subbands in bulk ZnO was confirmed by the detailed analysis of the Zeeman splitting of the free and bound excitons. The polarization properties and the angular dependence of the transition energies from excitons bound to ionized and neutral impurity centers indicated the Γ_7 character of the upper A valence band. The obtained Γ_7 effective g values are in good with theoretical calculations. We observed no low temperature PL transitions involving the Γ_9 hole states from the B valence subband.

ACKNOWLEDGEMENTS

The work of A. V. Rodina was carried out during the stay at the Institute for Solid State Physics, TU Berlin, and supported by the Deutsche Forschungsgemeinschaft (DFG).

REFERENCES

1. D. G. Thomas, *J. Phys. Chem.* **15**, 86 (1960).
2. Y. S. Park, C. W. Litton, T. C. Collins, and D. C. Reynolds, *Phys. Rev.* **143**, 512 (1966).
3. B. Segall, *Phys. Rev.* **163**, 769 (1967).
4. W. Y. Liang and A. D. Yoffe, *Phys. Rev. Lett.* **20**, 59 (1968).
5. K. Hümmer, *phys. stat. sol.* **56**, 249 (1973).
6. M. Rosenzweig, Diploma Thesis, TU Berlin, 1975.
7. G. Blattner, G. Kurtze, G. Schmieder, and C. Klingshirn, *Phys. Rev. B* **25**, 7413 (1982).
8. D. C. Reynolds, D. C. Look, B. Jogai, C. W. Litton, G. Cantwell, and W. C. Harsch, *Phys. Rev. B* **60**, 2340 (1999).
9. B. Gil, *Phys. Rev. B* **64**, 201310(R) (2001)
10. B. Gil, A. Lusson, V. Sallet, R. Triboulet, and P.Bigenwald, *Jpn. J. Appl. Phys. Lett.* **40**, L1089 (2001).
11. W. R. L. Lambrecht, A. V. Rodina, S. Limpijumnong, B. Segall, and B. K. Meyer, *Phys. Rev. B* **65**, 075207 (2002).
12. V. Val. Sobolev and V. V. Sobolev, *Lith. J. of Physics* **42**, 189 (2002).

13. K. Hazu, T. Sota, K. Suzuki, S. Adachi, SF. Chichibu, G. Gantwell, D. B. Eason, D. S. Reynolds, and C. W. Litton, Phys. *Rev. B* **68**, 033205 (2003).
14. A. V. Rodina, M. Strassburg, M. Dworzak, U. Haboeck, A. Hoffman, A. Zeuner, H. R. Alves, D. M. Hoffmann, and B. K. Meyer, *Phys. Rev. B* **69**, 125206 (2004).
15. B. K. Meyer, H. Alves, D. M. Hofman, W. Kriegseis, T. Riemann, J. Christen, A. Hoffmann, M. Strassburg, M. Dworzak, U. Haboeck, and A. V. Rodina, *phys. stat. sol. (b)* **241**, 231 (2004).
16. J. Gutowski, N. Presser, and I. Broser, *Phys. Rev. B* **38**, 9746 (1988).
17. G. Blattner, C. Klingshirn, R. Helbig, R. Meinl, *phys. stat. sol. (b)* **107**, 105 (1981).
18. P. Loose, M. Rosenzweig, and M. Wohlecke, *phys. stat. sol. (b)* **75**, 137 (1976).
19. D. C. Reynolds, C. W. Litton, and T. C. Collins, *Phys. Rev.* **140**, A1726 (1965).
20. D. C. Reynolds and T. C. Collins, *Phys. Rev.* **185**, 1099 (1969).
21. K. Thonke, N. Kerwien, A. Wysmolek, M. Potemski, A. Waag, and R. Sauer, *Mat. Res. Soc. Symp. Proc.* Vol. **719**, F2.4.1 (2002); K. Thonke, N. Kerwien, A. Wysmolek, M. Potemski, A. Waag, and R. Sauer, in Proc. 26th Int'l Conf. on the Physics of Semiconductors, edited by R. Long and J. H. Davies, Institute of Physics Publishing, Bristol (UK) and Philadelphia (USA), Institute of Physics Conference Series Number **171**, P22, (2003).
22. D. G. Thomas and J. J. Hopfield, *Phys. Rev.* **128**, 2135 (1962).
23. T. Skettrup, M. Suffczynski, and W. Gorzkowski, *Phys. Rev. B* **4**, 512 (1971).
24. A. V. Malyshev, I. A. Merkulov, and A. V. Rodina, *Fiz. Tverd. Tela* **40**, 1002 (1998) [*Physics of the Solid State* **40**, 917 (1998)].
25. H. Alves, D. Pfisterer, A. Zeuner, T. Riemann, J. Christen, D. M. Hofmann, and B. K. Meyer, *Optical Materials* **23**, 33 (2003).
26. M. A. Lampert, *Phys. Rev. Lett.* **1**, 450 (1958).
27. A. Zeuner, H. R. Alves, D. M. Hofmann, B. K. Meyer, A. Hoffmann, U. Haboeck, M. Strassburg, and M. Dworzak, *phys. stat. sol. (b)* **234**, R7 (2002).